JSR Publications

Available Online

J. Sci. Res. **6** (2), 217-231 (2014)

JOURNAL OF SCIENTIFIC RESEARCH

www.banglajol.info/index.php/JSR

Impact of Lithium Composition on Structural, Electronic and Optical Properties of Lithium Cobaltite Prepared by Solid-state Reaction

F. Khatun[a], M. A. Gafur[b], M. S. Ali[a], M. S. Islam[a], and M. A. R. Sarker[a,*]

[a]Department of Physics, Rajshahi University, Rajshahi-6205, Bangladesh

[b]Bangladesh Council for Scientific and Industrial Research (BCSIR), Kudrat-I-Khuda Road, Dhanmondi, Dhaka-1205, Bangladesh

Received 6 February 2014, accepted in final revised form 24 April 2014

Abstract

The lithium-cobalt oxide Li_xCoO_2 is a promising candidate as highly active cathode material of lithium ion rechargeable batteries. The crystalline-layered lithium cobaltite has attracted increased attention due to recent discoveries of some extraordinary properties such as unconventional transport and magnetic properties. Due to layered crystal structure, Li contents (x) in Li_xCoO_2 might play an important role on its interesting properties. $LiCoO_2$ crystalline cathode material was prepared by using solid-state reaction synthesis, and then Li_xCoO_2 (x<1) has been synthesized by deintercalation of produced single-phase powders. Structure and morphology of the synthesized powders were investigated by X-ray diffraction (XRD), Infrared spectroscopy, Impedance analyzer etc. The influence of lithium composition (x) on structural, electronic and optical properties of lithium cobaltite was studied. Temperature dependent electrical resistivity was measured using four-probe technique. While Li_xCoO_2 with x = 0.9 is a semiconductor, the highly Li-deficient phase ($0.75 \geq x \geq 0.5$) exhibits metallic conductivity. The ionic conductivity of Li_xCoO_2 (x = 0.5 – 1.15) was measured using impedance spectroscopy and maximum conductivity of $Li_{0.5}CoO_2$ was found to be 6.5×10^{-6} S/cm at 273 K. The properties that are important for applications, such as ionic conductivity, charge capacity, and optical absorption are observed to increase with Li deficiency.

Keywords: Calcination; Characterization; Inorganic compounds; Solid-State reaction; X-ray diffraction.

doi: http://dx.doi.org/10.3329/jsr.v6i2.17900 J. Sci. Res. **6** (2), 217-231 (2014)

1. Introduction

Recently, lithium-ion rechargeable batteries have been much studied for use as a power source of electric vehicles and various portable electronic devices because of their high power and high discharge voltages [1]. Now-a-days, one of the most promising power

* *Corresponding author*: razzaque_ru2000@yahoo.com

sources is the rechargeable lithium ion battery (LIB). High performance LLBs are favored in applications where low weight and small volume is desired, such as laptop computer, cellular phones and various portable electric appliances [2]. All solid-state LIBs using solid-inorganic materials have attracted attention owing to their safely and stability. Performance of the rechargeable batteries are determined by properties of the materials applied for their construction. In case of LIBs the most sensitive part of the device is cathode that may be formed of lithium with transition metal oxides [3]. Materials for cathodes in rechargeable LIBs have known a renewed research interest in recent years, both from the experimental and the theoretical point of view [4-6].

Lithium based layered transition metal oxides $LiMO_2$ (M = Ni, Co, Mn, Al, V) have attracted great interest worldwide and most studied for demand of high capacity energy storage devices. These materials are mainly used in lithium ion rechargeable batteries due to their attractive properties such as high energy density, high average output voltage, exceptional cycling behavior, high rate capability and wide working temperature ranges. Among this group, $LiCoO_2$ is one of the most promising materials for commercial application because of its favorable features such as good capacity, excellent electrochemical stability, good power rates, low self-discharge, and excellent life cycle [7]. The structural stability of the $LiCoO_2$ cathode material is such that the layered cation ordering extremely preserved even after a repeated process of insertion and extraction of Li^+ ions [8]. This topotactic Li-intercalation mechanism is the basis for the materials application of $LiCoO_2$ as an electrode in a rechargeable battery [9].

$LiCoO_2$ crystals in particular have attracted attention due to their layered structure because Li^+ ions are easily removed from $LiCoO_2$ structure [7]. This layered crystallographic structure is able to accommodate foreign cations in a reversible way, without drastic change of solid matrix. The excess charge created during battery performance is compensated by electrons provided to or removed from the matrix. This is possible for relatively easy change of valence state of transition metal ion in $LiCoO_2$. The amount of energy stored in the battery depends on the charge (Li^+ ions) in the structure of cathode material [3]. The electronic properties of Li_xCoO_2 are sensitively influenced by the Li content (x) [10]. For a long Li non-stoichiometry range, Li_xCoO_2 would display a mixed electronic/ionic (Li^+) conductivity, consistent with the requirements of electrochemical cathode material. Until now, some interesting structural and electronic properties of this important cathode material are open questions. We want to realize more and more into the structural and electronic and optical properties of Li_xCoO_2.

Properties of $LiCoO_2$ are depends on the conditions of synthesis and subsequent processing. Many methods have been applied for preparation of $LiCoO_2$ crystals such as hydrothermal growth, sol-gel, co-precipitation, pulsed laser deposition, electrostatic spray deposition and solid-state synthesis methods. However, these methods except solid-state reaction route require different difficult conditions or large quantity of solvent and organic materials [11]. There are several disadvantages in hydrothermal growth technique such as expensive equipment and high total cost. For sol-gel crystallization, the grown $LiCoO_2$ crystals have a poor crystallinity [7]. Currently, $LiCoO_2$ has often been synthesized by conventional high temperature solid-state reaction route in factories because this is the most convenient method [12]. In our study, $LiCoO_2$ of high activity as cathode materials

with high purity and crystallinity have been prepared by solid-state reaction technique.

In this work, we discuss the effects of lithium non-stoichiometry on the structural, electronic and optical properties of Li_xCoO_2. The efficiency of this material as cathode depends on grain size, dislocation density and micro strain. The performance of this cathode material also depends on electrical and ionic conductivity at ambient and high temperature. Studies on the conductivity of delithiated $LiCoO_2$ cathode materials are important to achieve improvement on the ionic conduction mechanism especially in its usage for lithium ion batteries. We showed the change of such conduction properties with Li non-stoichiometry. Further we investigated the variation of charge capacity, dielectric constant, electrical impedance and optical absorption with Li contents in Li_xCoO_2.

2. Experiment

High-purity (>99.99%) powders of Li_2CO_3 and Co_3O_4 were used as the starting material for preparation of $LiCoO_2$. Initially we studied the phase formation employing a thermobalance (TG/DTA 630) in order to establish the procedure for synthesizing Li_xCoO_2. A stoichiometric mixture of Li_2CoO_3 and Co_3O_4 with molar ratio of Li:Co = 1:1 *i.e.* x = 1.0, was heated in an air atmosphere with a heating program as shown in the inset of Fig. 1. A representative thermogravimetric (TG) curve obtained for the raw material mixture is shown in Fig. 1. From this thermal analysis, it was found that the weight loss between 500 and 790 °C is too large due to decarbonation of raw materials followed by the equation $Li_2CoO_2 \rightarrow Li_2O + CO_2$. Endothermic peak at around 710 °C in differential thermal analysis (DTA) curve indicates the decomposition of Li_2CO_3 and exothermic peak at around 790 °C indicates the formation of $LiCoO_2$ as a result of reaction between Li_2O and Co_3O_4. This suggest that at temperature lower than ~ 500 °C, the chemical reaction between the raw materials may not be active yet and there is no weight change above 790 °C where the phase formation is completed.

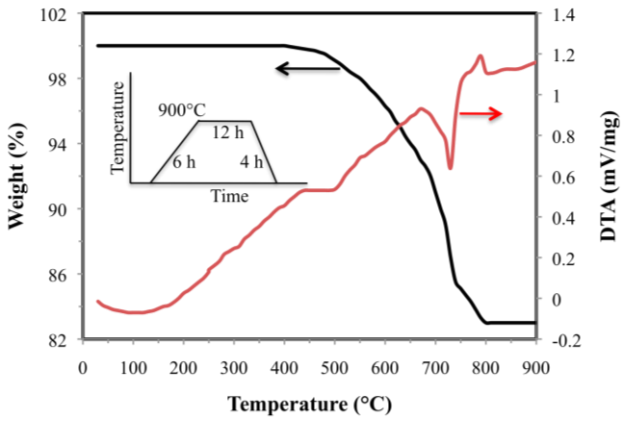

Fig. 1. Thermogravimetric curve for the phase formation process of $LiCoO_2$.The inset represents the heating program employed.

At the first step of synthesis, the reactants were dried in air in an oven at 100 °C for12 h. A powdered mixture of Li_2CO_3 and Co_3O_4 with molar ratio of Li:Co = 1.1:1 *i.e, x* = 1.1, was mixed well in an agate mortar using ethanol, than dried and calcined at 800 °C for 24 h in an air atmosphere. A 10 % molar excess of Li_2CO_3 (x = 1.1) was added in the mixture to compensate loss due to Li evaporation at high temperature. Before the next heat treatment, the powder was reground thoroughly to ensure homogeneity. The powder was calcined again at 850°C for 12 h in an air atmosphere. After second heat treatment, the powder was grounded and pelletized in 12 mm diameter under pressure of 60 KN using pressure gauze. The compressed pellets were sintered at 950°C for 12 h in an air atmosphere. In all heat treatments, the temperature rising and cooling rates were 3 °C/min. Li rich composition $Li_{1.05}CoO_2$ and $Li_{1.15}CoO_2$ were prepared in the same way of stoichiometric $LiCoO_2$ sample. For preparation of Li deficient composition Li_xCoO_2 ($0.5 \geq x \geq 1.0$), the stoichiometric powder, $LiCoO_2$ was deintercalated using mixture of liquid Br_2 and acetonytrile. In the deintercalation process, 10 g samples of stoichiometric $LiCoO_2$ were reacted with different amounts of liquid Br_2 according to the relation $x = 0.441 + 0.846/(R+ 1.454)$, R is the molar ratio of Br_2 to $LiCoO_2$, and x is the lithium content of the deintercalated compound. This equation was derived from ICP-AES analysis of $LiCoO_2$ synthesized by Hertz *et al*. [13]. The lithium composition was analyzed by using atomic absorption spectroscopy.

The powder samples were analyzed by X-ray diffraction (XRD) using a CuK_α (λ = 0.154 nm) radiation source using a Rigaku HYGD Multiflex X-ray diffractometer at room temperature in center for crystal science and technology, Japan. The diffraction angle (2θ) range between 5° and 85° was scanned. Fourier transform infrared (FTIR) spectrophotometer (Spectrum 100, Perkin Elmer) was used for FTIR transmission spectrum of the powder samples. Resistivity measurements were carried out by the conventional four-probe method. Fine polishing was done for the disc like samples. The Agilent Precision Impedance Analyzer (Agilent technologies, Model: 4294A Japan) was used for measurements of frequency dependences ac conductance, impedance, dielectric constant and capacitance. The ionic conductivity was calculated from the complex impedance using Nyquist plot. The samples were characterized by UV–Visible spectrophotometer (Shimazu: UV–1650 PC) for wavelength dependence absorption spectrum.

3. Results and discussions

3.1 *Structural properties*

Crystalline $LiCoO_2$ powder was obtained by conventional solid-state reaction technique with a final firing at 850 °C. The powder samples of Li_xCoO_2 with x = 0.5 –1.15 were characterized at the room temperature by a Rigaku Mutiflex diffractometer range from 2θ = 5° to 85° with CuK_α radiation (λ = 1.5418 Å), at 40 KV and 30 mA. The unit cell refinement was accomplished using XRD data and CellCal software. Typical XRD

patterns of Li_xCoO_2 crystalline powders shown in Fig. 2 reveals that all these materials are single phase with trigonal crystal structure of hexagonal symmetry, space group R3m. The hexagonal layer structure is maintained in the range of $0.5 \leq x \leq 1.15$ in Li_xCoO_2. The prepared samples were identified as highly crystalline and homogeneous by indexing these XRD patterns using JCPDS data No. 44-0145. Here the sharp peaks indicate the good crystallinity. In the XRD pattern the impurity phase peaks of Co_3O_4 and Li_2CoO_3 are negligible, so the pure phase solid is obtained, which indicates that $LiCoO_2$ can be synthesized fast by conventional solid-state reaction route. The good crystallinity of $LiCoO_2$ crystals would improve the rate capability of Li-ion cells.

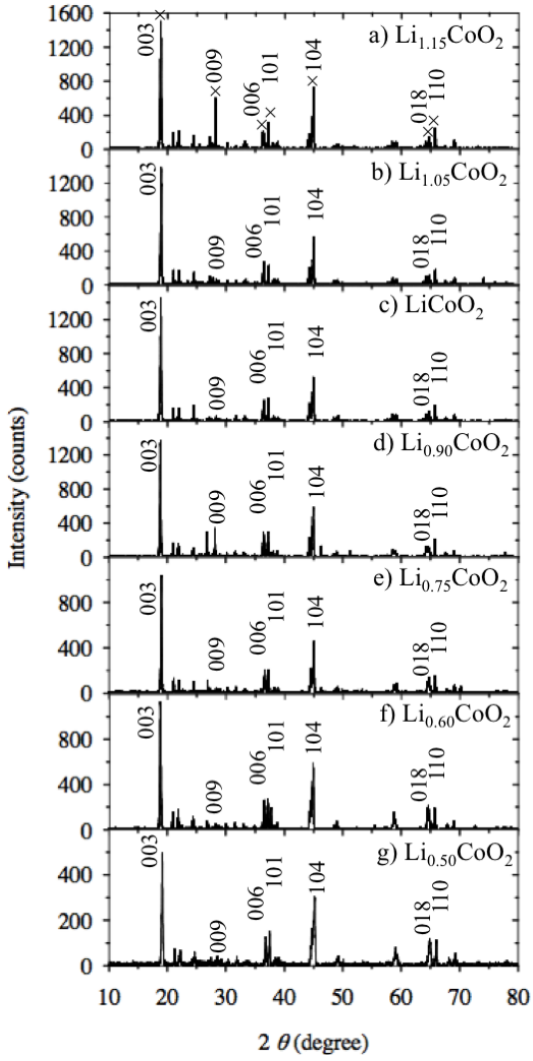

Fig. 2. X-ray diffraction patterns of the Li_xCoO_2 samples (x = 0.5–1.15).

In the XRD patterns, (003) peaks indicates the property of layer structure of $LiCoO_2$, (104) peaks indicates the property of basic unit of Co-O-Co bond which form this kind of layer compound, and the intensity ratio of (003) and (104) peaks indicates the perfection of crystallization [12]. The larger value of intensity ratio demonstrates the better crystallinity [14]. The relative intensity of main peaks decreases with increase or decrease of x value in Li_xCoO_2. The table 1 lists the lattice parameters obtained from indexing of XRD pattern using CellCal program and corresponding intensity ratios of main peaks.

Table 1. Lattice parameters derived from X-ray diffraction data and ratio of main XRD peaks.

x in Li_xCoO_2	a (Å)	c (Å)	c/a	I_{003}/I_{104}
1.15	2.8258	14.1667	5.013273	2.068
1.05	2.8389	14.2559	5.021462	2.479
1.00	2.8332	14.2476	5.028691	2.788
0.90	2.8359	14.3161	5.048725	2.314
0.75	2.8345	14.3577	5.065323	2.275
0.60	2.8321	14.3603	5.070623	1.929
0.50	2.8378	14.3899	5.070815	1.631

The calculated lattice parameters are approximately equal to the standard lattice constants obtained from the JCPDS card no. 44-0145. The layer structure of $LiCoO_2$ is shown in Fig. 3. The lattice parameter 'c' increases with reduction of Li contents (x) in Li_xCoO_2 while lattice parameter 'a' shows opposite variation. This is consistent with the removal of lithium from $LiCoO_2$, which leads to an increase of the spacing between layers due to repulsive forces between negatively charged oxygen ions [15]. Consequently, this results in expansion of the structure in the direction parallel to the c axis [16].

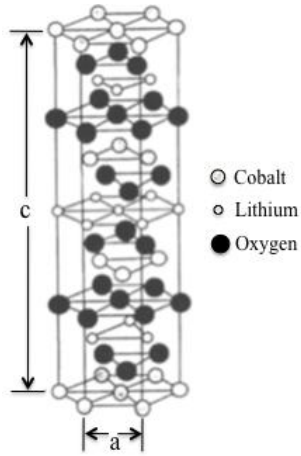

Fig. 3. Crystallographic stricture of trigonal elementary cell of $LiCoO_2$ (R3m space group, hexagonal symmetry).

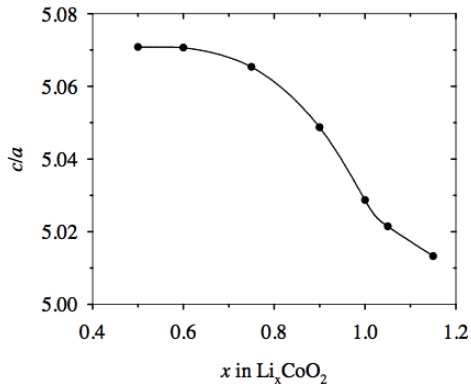

Fig. 4. Variation of the lattice parameter ratio *c*/*a* with *x* value in Li_xCoO_2.

The observed slight decrease in lattice parameter '*a*' can be explained by the oxidation of the Co^{3+} ions and formation of Co^{4+} ions. The lattice parameter ratio c/a increases with decrease of Li contents (*x*) as shown in the Fig. 4. As the distance between two CoO_2 layers is indicated by the value of *c*/*a*, this also expresses the expansion of unit cell along c direction. The larger value of *c*/*a* implies the structure to be more flexible to deintercalation/intercalation of Li^+ from $LiCoO_2$ [17].

The cation ordering in the crystal structure of cathode material is one of the most important factors for good performance that is measured by the intensity ratio of main peaks in the XRD patterns. Integrated intensity ratio of (003)/(104) peaks has been considered to be an important factor indicating the degree of cation ordering in the crystal structure of lithium cobalt oxides [18,19]. It has been proposed that the electrochemical performance of Li_xCoO_2 cathode material is remarkably improved when the (003)/(104) peaks intensity ratio is higher than 1.2 [20-22]. The intensity ratios of main peaks are shown in Table1 that were more than 1.6 for all values of *x* in Li_xCoO_2. This reveals that the ordering of Li and Co is remain unchanged during the Li extraction from the sample. On the other hand, the intensity ratio between (003) and (104) reflections decrease significantly due to Li extraction. This suggests that the cobalt ions present in the Li planes are extracted along with Li during the oxidation reaction. All diffraction patterns show that the (006) – (101) and (108) – (110) peak doublets are well defined and separated. This suggests a dimensionally stable structure with a highly ordered distribution of cations in the lattice [23, 24].

The performance of the lithium ion battery is affected by a numerous factors such as anode and cathode particle size (*D*), micro strain (ε) and dislocation density (δ) [25]. The average grain size (*D*) and micro strain (ε) of the Li_xCoO_2 particles were calculated using Scherrer formulae, $D = \frac{0.94\lambda}{\beta\cos\theta}$ [26] and $\varepsilon = \frac{\beta}{4\tan\theta}$ [27], respectively, where λ is the X-ray wave length (1.5418 Å), 0.94 is the crystal shape constant, θ is the reflection angle of the highest peak and β is the full width at half maximum (FWHM) of the highest peak in radians. The dislocation density (δ) of the Li_xCoO_2 was estimated using the equation

$\delta = \frac{1}{D^2}$ (lines/m^2) [28]. The calculated D, δ and ε values are listed in Table 2.

Table 2. Grain size, defect density and micro strain derived from X-ray diffraction data.

x in Li_xCoO_2	*D* (nm)	$\delta \times 10^{14}$ (lines/m^2)	$\varepsilon \times 10^{-3}$ (lines.m^{-4})
1.15	50.956	3.851	4.346
1.05	45.676	4.793	4.823
1.00	50.261	3.957	4.390
0.90	52.159	3.676	4.241
0.75	61.119	2.677	3.589
0.60	45.867	4.753	4.836
0.50	41.559	5.789	5.243

The obtained values are comparable to the reported results ofS/cm Yilmaz *et al*. [25]. The dislocation density (δ) indicates the length of dislocation lines per unit volume and measures the amount of defects in a crystal. The values of *D*, δ and ε decrease with decrease of Li content (*x*) in the Li_xCoO_2 although there is some discontinuity. It means the quality of the lithium cobaltite cathode material improved for delithiation effect.

In order to get physical insight of the chemical bonding and phase formation, we also studied the structure by Fourier transform infrared (FTIR) spectroscopy. FTIR spectroscopic technique is powerful for investigating the local structure and cation environment in oxides [29, 30]. The results of FTIR spectroscopic analysis are shown in the Fig. 5. The main spectrum of $LiCoO_2$ contains the following main absorption bands: 227, 515, 626, 1024, 1384, 1633 and 3435 cm^{-1}. These results confirm the XRD observations showing that the vibration bands for precursors vanished and the vibration bands for the oxide network developed.

In the far-infrared region, we observed the single well-resolved band at 227 cm^{-1}. This sharp band in $LiCoO_2$ is assigned due to an asymmetric stretching motion of the LiO_6 octahedra [31]. It is the unique finger print of the Li site occupancy in the trigonal structure. From the spectra shown in the Fig. 5 it is clear that (i) extracting Li ions does not change the space group, (ii) the frequency of the LiO_6 octahedra is affected by lithium deintercalation, and (iii) the displacement of the stretching peaks occurs. The slight frequency shift of LiO_6 vibrations (227 cm^{-1} to 225 cm^{-1}) implies that the octahedral oxygen environment of Li+ ions remains quite stable in the delithiated structure.

The strength of LiO_6 peaks increase upon Li extraction due to density of oscillators. The broadening of all IR bands is associated with the disorder induced by the departure of the Li ions located between two CoO_2 blocks. The broadening of the low frequency band is also attributed to the random distribution of Li ions remaining in the host matrix. A

slight frequency shift is observed for the high-wave number bands which are assigned to the CoO_6 vibrations. This also corresponds to the repulsive interactions between the two adjacent negatively charged CoO_2 layers upon deintrcalation. Thus we can conclude that the CoO_2 layers are not strongly affected by the lithium deintercalation process. The increase of the absorbance of the Li_xCoO_2 sample can be attributed to the change in the electrical conductivity of the material. This suggests the existence of collective delocalized electrons. These results agree well with the data of electrical measurements, which show that $LiCoO_2$ has a semiconductor like conductivity and Li_xCoO_2 exhibits almost temperature dependent conductivity. There is a sharp medium absorption peaks around 1384 cm^{-1}, which is due to the vibrations of the lithium cobaltite crystal lattice. The results of FTIR analysis were good agreement with XRD results.

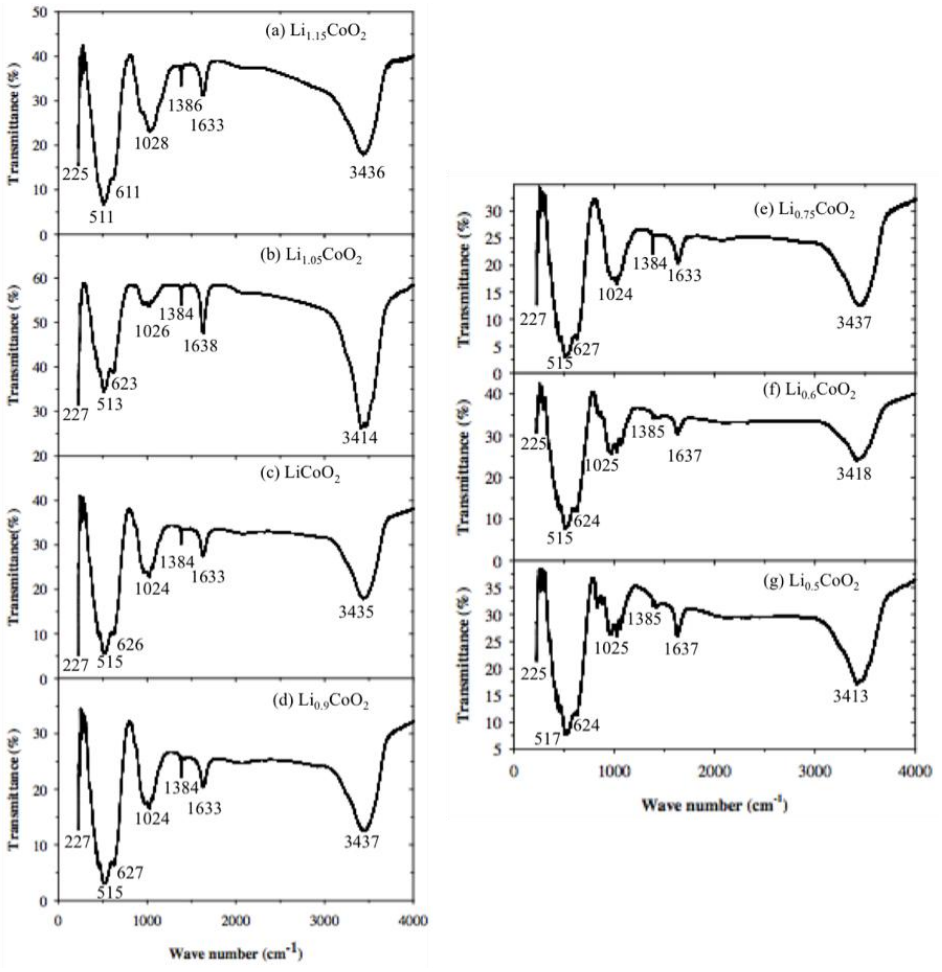

Fig. 5. FTIR spectrum of Li_xCoO_2 samples (x = 0.5–1.15).

4.2. *Electronic properties*

The most important property of the electrode material $LiCoO_2$ is its ability to change stoichiometry and, specially, its lithium content within the same structure. The electrochemical change of non-stoichiometry may be expressed by the equation: $LiCoO_2 \leftrightarrow Li_xCoO_2 + (1\text{-}x)Li$, where Li_xCoO_2 is lithium deficient composition, forming cathode, and $(1–x)Li$ represents the amount of lithium that is transferred to anode. In the commercial batteries, the lithium content x in Li_xCoO_2 varies between 1 and 0.5. In this range the structure of $LiCoO_2$ remains unchanged and the battery's performance is reversible [32]. From this point of view, the electrical conductivity of lithium cobaltite may depends on the Li non stoichiometry *i.e*. lithium content x [29]. In this work we showed the variation of electrical resistivity with x (x = 0.5 – 1.15) in Li_xCoO_2.

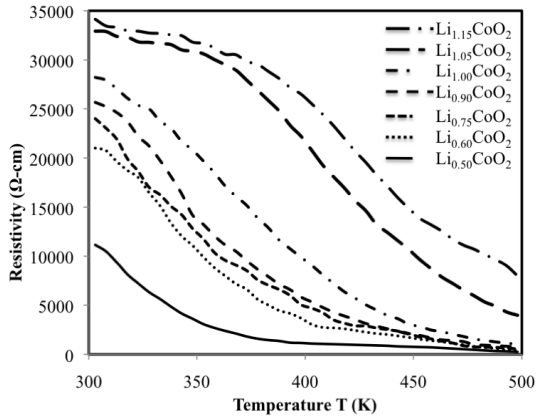

Fig. 6. Temperature dependence electrical resistivity of Li_xCoO_2 samples (x = 0.5–1.15).

The temperature dependence dc resistivity of the samples was measured using four-probe technique from room temperature to 500 K as shown in Fig.6. The electrical resistivity decreases with decreasing Li content (x) in Li_xCoO_2 which indicates that the electrical conductivity increases for delithiation effect. The results reveal that the resistivity of $LiCoO_2$ is three times larger than that of $Li_{0.5}CoO_2$. It indicates that Li_xCoO_2 (x > 0.5) are semiconductors whereas $Li_{0.5}CoO_2$ is a metallic semiconductor. The dc resistivity strongly depends on the temperature. The ac conductance of the samples were measured by impedance analyzer, where the signal frequency was varied from 100 kHz to 10 M Hz and oscillating voltage 300 mV was applied. Fig. 7 shows the frequency dependence ac conductance of Li_xCoO_2 samples where the ac conductance increases with frequency for all the samples. The frequency response ac conductance also depends on the Li nonstoichiometry of Li_xCoO_2 samples. The ac conductance of stoichiometric $LiCoO_2$ is lower than all non stoichiometric samples. The ac conductance of $Li_{1.15}CoO_2$ and $Li_{1.05}CoO_2$ are very close to $LiCoO_2$ while that of Li deficient composition is significantly large. The efficiency of cathode materials of the rechargeable batteries depends on the ac

conductivity. This result indicates that the Li non stiochiometry of Li_xCoO_2 strongly affects the efficiency of the Li-ion cells [9].

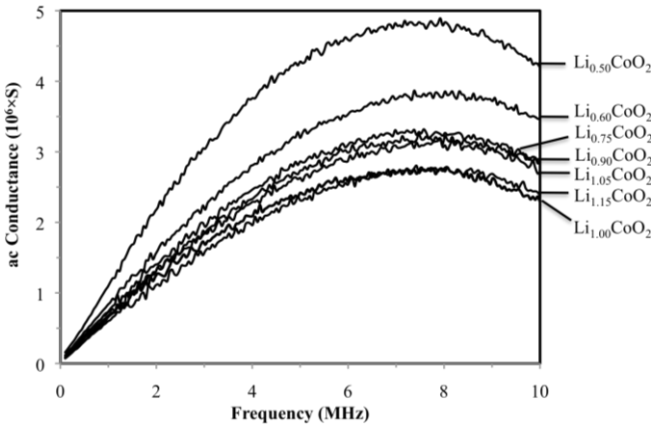

Fig. 7. Frequency dependence ac conductance of Li_xCoO_2 samples (x = 0.5–1.15).

The ionic conductivity of the samples was calculated by measuring the frequency dependence impedance using precision impedance analyzer. The ionic conductivity could be calculated using the Nyquist impedance plot of imaginary part (Z″) versus real part (Z′) of complex impedance [33]. The complex impedance plot shows a well-defined semi-circle in the high frequency region, which is due to bulk effect of the electrodes. The point where the semi-circle tends to intersect the real axis (Z′) gives the value of bulk resistance R_b. Inset of Fig. 8 shows the Nyquist complex impedance plot of $Li_{0.5}CoO_2$ from which the bulk resistance, R_b was obtained directly. By knowing the value of bulk resistance (R_b) and the dimensions of the sample, the ionic conductivity was calculated by using the relation:

$\sigma = \frac{d}{R_b A}$, where d is the thickness and A is the surface area of the sample [34].

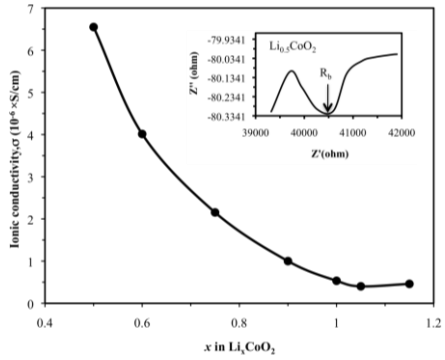

Fig. 8. Ionic conductivity of Li_xCoO_2 samples (x = 0.5–1.15).

Fig. 8 shows the ionic conductivity of the Li_xCoO_2 samples for different Li contents (x). The ionic conductivity increased for delithiation effect of $LiCoO_2$ and maximum conductivity of 6.5×10^{-6} S/cm was obtained for the composition $Li_{0.5}CoO_2$. The high ionic conductivity in an electrode is attributed to increased ionic mobility and increased ionic charge carrier concentration.

4.3. *Optical properties*

The optical properties of a material is very important in some applications such as optical coatings, reflectors, absorbers and various optoelectronic devices. The dielectric property of a material is another important factor in electronic device applications.

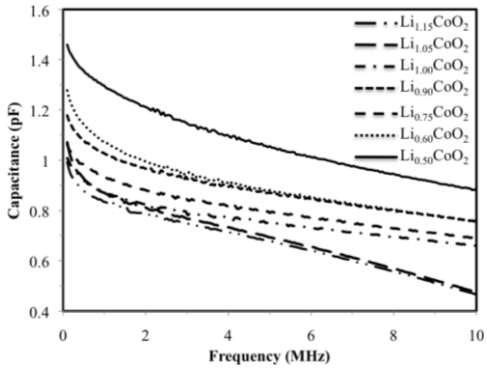

Fig. 9. Frequency dependence capacitance of Li_xCoO_2 samples (x = 0.5–1.15).

We evaluate the optical and dielectric properties of lithium cobaltite, Li_xCoO_2 as a function of Li composition (x). Dielectric properties of the Li_xCoO_2 samples were measured by precision impedance analyzer. Silver paste was coated on both surface of each sample before measurement. Dielectric constant is a measure of materials ability to store electric charge. The frequency dependence capacitances of samples were measured within the frequency ranges 100 kHz to 10 MHz at room temperature as shown in Fig. 9. The capacitance of Li_xCoO_2 is high at low frequency region and decreases with increase of frequency for all samples. The capacitance of Li_xCoO_2 is high at low frequency region due to contribution of all kinds of polarization at low frequency, then decreases with increase of frequency and finally approaches to all most constant value above 12 MHz. This is due to the change of space charge, ionic and orientation polarization at higher frequencies [35]. The capacitance of Li_xCoO_2 is lowest for x = 1.15 and increases with decrease of x value. This means that the charge capacity of the lithium cobaltite cathode increases with decrease of lithium content. Fig. 10 shows the frequency dependence dielectric constant of Li_xCoO_2 samples that implies the same tendency of capacitance. Frequency response capacitance and dielectric constant strongly depends on the Li nonstoichiometry in the Li_xCoO_2 samples.

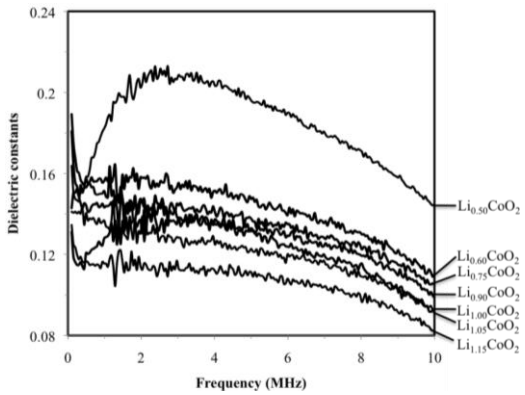

Fig. 10. Frequency dependence dielectric constants of Li_xCoO_2 samples (x = 0.5–1.15).

The reported results on optical absorption or transmission of bulk $LiCoO_2$ are not available. Rao [36] investigated the optical properties of $LiCoO_2$ thin films using Hitachi U 3400 UV-VIS-NIR double beam spectrophotometer. He recorded the optical absorption spectra in the wavelength range 300 – 1200 nm and the absorption peak was found near at 850 nm. In this study, UV-Visible absorption spectrum of the Li_xCoO_2 samples was recorded by using a UV-Vis spectrophotometer (Shimazu: UV–1650 PC) in the photon wavelength range 200 – 800 nm. Fig.11 shows the absorption spectrum of Li_xCoO_2 samples. The absorption slightly increases with increase of wavelength in the visible region. There are some absorption peaks in the ultraviolet region for most of the samples. There are two very strong absorption peaks at 236 nm and 274 nm for the $Li_{0.75}CoO_2$ sample. There are two strong absorption peaks at 208 nm and 216 nm and a medium peak at 269 nm for the $Li_{0.9}CoO_2$ sample. There are single weak peaks at 201 nm for $LiCoO_2$, at 203 nm for $Li_{0.6}$ CoO_2 and at 202 nm for $Li_{0.5}CoO_2$ samples. These peaks reveal the absorption criteria of lithium cobaltite in the ultraviolet – visible region depending on the Li deficiency. There are no peaks observed for Li rich composition $Li_{1.05}$ CoO_2 and $Li_{1.15}$ CoO_2 in the absorption spectrum. This result reveals that stoichiometric $LiCoO_2$ is not a strong absorber but for delithiation its absorptive power increases. Lithium cobaltite might be used as absorber after deintercalation.

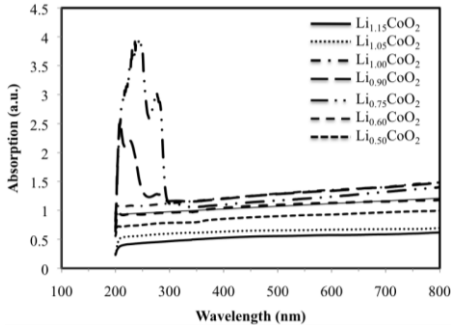

Fig. 11. The UV–Visible absorption spectrum of of Li_xCoO_2 samples (x = 0.5–1.15).

5. Conclution

Lithium cobaltite ($LiCoO_2$) single-phase powders have been successfully prepared by solid-state reaction technique. This technique is most effective to control precisely the Li contents in the $LiCoO_2$ samples by avoiding unwanted Li evaporation during synthesis procedure. The Li deficient compositions (Li_xCoO_2) were successfully prepared by deintercalation of $LiCoO_2$ single-phase power. The phase formation condition was fixed by thermal analysis and single crystalline phase was confirmed by XRD analysis. With varying the Li concentration (x) in the Li_xCoO_2 samples, structural, electronic and optical properties were reported first by various experimental techniques. The structural, electrical and optical measurements reveal that its all properties are well agreements with literature. We reported that the crystal of lithium cobaltite remain unchanged upon Li extraction. The electrical resistivity decreased for delithiation effect and minimum resistivity of 1.1×10^4 Ω-cm was obtained for the composition $Li_{0.5}CoO_2$. The ionic conductivity enhanced for delithiation effect of $LiCoO_2$ and maximum conductivity of 6.5×10^{-6} S/cm was obtained for the composition $Li_{0.5}CoO_2$. In this article, we evaluated the Li non stoichiometric effects of $LiCoO_2$ on crystal quality, grain size, micro strain, defect density, charge capacity and optical absorption in first time. We reported that the micro strain and defect density decreased for extraction of Li^+ from $LiCoO_2$. We also demonstrated that the properties, responsible for high efficiency of $LiCoO_2$ cathode materials, improved for Li^+ extraction. Further we want to propose here that the performance of Li-ion rechargeable batteries increased for delithiation of $LiCoO_2$ cathode materials.

Acknowledgements

This work was partially supported by the Rajshahi University Research Grant (No. A 774). The authors would like to thank Mr. Md. Saiful Islam, Senior Scientific Officer, Central Science Laboratory, Rajshahi University, for facilitating experimental works. Further the authors thank Bangladesh Council for Scientific and Industrial Research authority and the Center for Crystal Science and Technology authority for providing experimental facilities.

References

1. J. M. Tarascon, M. Armand, Nature **414**, 359 (2001). http://dx.doi.org/10.1038/35104644
2. C. H. Han, Y. S. Hong, C. M. Park, and K. Kim, J. Power Sources **92**, 95 (2001). http://dx.doi.org/10.1016/S0378-7753(00)00505-X
3. T. Bak, J. Nowotny, M. Rekas, C. C. Sorrell, and S. Sugihara, Ionics **6**, 92 (200).
4. M. Catti, Phys. Rev. B, **61**, 1795 (2000). http://dx.doi.org/10.1103/PhysRevB.61.1795
5. R. Koksbang, J. Barker, H. Shi, and M. Y. Saidi, Solid State Ionics **84**,1 (1996). http://dx.doi.org/10.1016/S0167-2738(96)83001-3
6. M. M. Thackeray, J. Electrochem. Soc. **142**, 2558 (1995). http://dx.doi.org/10.1149/1.2050053
7. K. Teshima, S. H. Lee, Y. Mizuno, H. Inagaki, M. Hozumi, K. Kohama, K. Yubuta, T. Shishido, and S. Oishi, Cryst. Growth Design **10**, 4471 (2010). http://dx.doi.org/10.1021/cg100705d

8. L. Predoana, A. Barau, M. Zaharescu, H. Vasilchina, N. Velinova, B. Banov, and A. Momchilov – Advanced Techniques for $LiCoO_2$ Preparation and Testing, Proceedings of the International Workshop "Advanced Techniques for Energy Sources Investigation and Testing" 4–9 Sept. 2004, Sofia, Bulgaria.
9. M. K. Aydinol, A. F. Kohan, and G. Ceder, Phys. Rev. B, **56**,1354 (1997). http://dx.doi.org/10.1103/PhysRevB.56.1354
10. T. Motohashi, Y. Sugimoto, Y. Masubuchi, T. Sasagawa, W. Koshibae, T. Tohyama, H. Yamauchi, and S. Kikkawa, Phys. Rev. B, **83**,195128 (2011). http://dx.doi.org/10.1103/PhysRevB.83.195128
11. Q. Dong, N. Kumada, Y. Yonesak, T. Takei, N. Kinomura, J. Ceram. Soc. Japan **119**, 538 (2011). http://dx.doi.org/10.2109/jcersj2.119.538
12. H. Guo-rong, L. Gang, P. Zhong-dong, X. Jin, Z. Xin-lon, and Y. Xiao-yuan, J. Cent. South Univ. Technol. **11**, 261 (2004). http://dx.doi.org/10.1007/s11771-004-0053-y
13. J. T. Hertz, Q. Huang, T. McQueen, T. Klimczuk, J. W. G. Bos, L. Viciu, and R. J. Cava, Phys. Rev. B **77**, 075119 (2008). http://dx.doi.org/10.1103/PhysRevB.77.075119
14. L. Jing, W. Zhaoyin, and W. Meimei, J. Inorg. Materials **17**, 1157 (2002).
15. L. P. Gaudart, V. C. Ciomaga, O. Dragos, R. Guillot, and N. Dragoe, J. Cryst. Growth **334**,165 (2011). http://dx.doi.org/10.1016/j.jcrysgro.2011.07.024
16. Y. Takahashi, N. Kijima, K. Dokko, M. Nishizawa, I. Uchida, and J. Akimoto, J. Solid State Chem. **180**, 31 (2007). http://dx.doi.org/10.1016/j.jssc.2006.09.018
17. Y. H. Wei, H. X. Jie, and C. L. Quan, J. Power Sources **81-82**, 637 (1999). http://dx.doi.org/10.1016/S0378-7753(99)00235-9
18. S. S. Mohammad and S. Asgari, J. Nanomater. **8**, 2010 (2010).
19. J. R. Dahn, V. von Saken, and C. A. Michal, Solid State Ionics **44**, 87 (1990). http://dx.doi.org/10.1016/0167-2738(90)90049-W
20. Y. Hao, Q. Lai, Z. Xu, X. Liu, and X. Ji, Solid State Ionics **176**, 1201 (2005). http://dx.doi.org/10.1016/j.ssi.2005.02.010
21. S. Sivaprakash, S. B. Majumder, S. Nieto, and R. S. Katiyar, J. Power Sources **170**, 433 (2007). http://dx.doi.org/10.1016/j.jpowsour.2007.04.029
22. S. J. Jin, K. S. Park, M. H. Cho, C. H. Song, A. M. Stephan, and K. S. Nahm, Solid State Ionics **177**, 105 (2006). http://dx.doi.org/10.1016/j.ssi.2005.08.015
23. S. A. Needham, G. X. Wang, H. K. Liu, V. A. Drozd, and R. S. Liu, J. Power Sources **174**, 828 (2007). http://dx.doi.org/10.1016/j.jpowsour.2007.06.228
24. H. Wang, Y. I. Jang, B. Huang, D. R. Sadoway, and Y. M. Chiang, J. Electrochem. Soc. **146**, 473 (1999). http://dx.doi.org/10.1149/1.1391631
25. M. Yilmaz, S. Aydin, G. Turgut, R. Dilber, and M. Ertuğrul, Prog. Nanotech. Nanomater. **1 (1)**, 5 (2012).
26. M. Yilmaz, G. Turgut, S. Aydin, and M. Ertugrul, J. Chem. Soc. Pak. **34**, 283 (2012).
27. K. Rajasekar, L. Kungumadevi, A. Subbarayan, and R. Sathyamoorthy, Ionics **14**, 69 (2008). http://dx.doi.org/10.1007/s11581-007-0146-3
28. K. Ravichandran, G. Murugananthan, and B. Sakthivel, Physica B: Condensed Matter **404**, 4299 (2009). http://dx.doi.org/10.1016/j.physb.2009.08.017
29. N. Amdoun, P, H. Zarrouk, and C. M. Julienb, Ionics **9**, 47 (2003).
30. C. Julien, Solid State Ionics **887**,136 (2000).
31. C. Julien, NATO Science Series **309**, 3 (2000).
32. M. Menetrier, I. Saadoune, S. Levasseur, and C. Delmas, J. Mater. Chem. **9**, 1135 (1999). http://dx.doi.org/10.1039/a900016j
33. X. Qian, N. Gu, Z. Cheng, X. Yan, E. Wang, and S. Dong, J. Solid State Electrochem. **6**, 8 (2001). http://dx.doi.org/10.1007/s100080000190
34. A. R. Polu and R. Kumar, Bull. Mater. Sci. **34**, 1063 (2011). http://dx.doi.org/10.1007/s12034-011-0132-2
35. W. D. Kingegy, Introduction to Ceramic (John Wilely & Sons, New York, 1960).
36. M. C. Rao, Int. J. Pure Appl. Phys. **6**, 365 (2010).